# Metal Binder Jetting of Superalloy Turbine for Turbocharger Application

Mattia Forgiarini [a,*], Fredrik Berg Lissel [b], Chad Beamer [c], Tim Noronha [d], David Sponseller [e]

[a] Azoth LLC, Ann Arbor, MI 48108, United States - *mattia@azoth3d.com (* Corresponding author)*
[b] Digital Metal AB, Höganäs, 263 39, Sweden - *fredrik.berglissel@digitalmetal.tech*
[c] Quintus Technologies LLC, Lewis Center, OH 43035, United States - *chad.beamer@quintusteam.com*
[d] Turbocam Inc, Barrington, NH 03825, United States - *tim.noronha@turbocam.com*
[e] OMNI Metals Lab Inc, Ann Arbor, MI 48108, United States - *dsponseller@omnimetalslab.com*

## Abstract

Metal Binder Jetting is a promising Additive Manufacturing technique as it can be used to form complex geometries out of almost any type of powder, without the use of heat input, at high production rates and low manufacturing cost. In this work, Metal Binder Jetting printing is explored as a fabrication process for a turbine composed of a Ni-base superalloy for a turbocharger application. Conventional wrought and machining methods used to manufacture turbines to date offer good mechanical properties for end-application performance, however, the high material "buy-to-fly" ratio has drawn interest to explore Additive Manufacturing approaches. Fusion-based Additive Manufacturing technologies, such as laser and electron beam powder bed fusion, are limited with respect to deposition rates and are challenged to print high gamma prime/gamma double prime strengthened Ni-base alloys due to their poor weldability. For these reasons, the development of 3D printing and post-processing approaches using fusionless Metal Binder Jetting for MAR-M-247 was investigated. Conventional post-process Hot Isostatic Pressing (HIP), and heat treatment were applied to establish baseline microstructural and mechanical property data along with the evaluation of an over-speed turbine spin test. Results were then leveraged to establish process-structural-property relationships for further optimization of the microstructure through post-process combined HIP and solution heat treatment, referred to as high pressure heat treatment (HPHT$^{TM}$), to maximize part performance.

## 1. Introduction

### 1.1 Review of Metal Binder Jetting Additive Manufacturing

Additive Manufacturing, also known as 3D printing, is a manufacturing method of joining material together, usually layer by layer, to make objects from digital three-dimensional model data. Metal Binder Jetting is an additive manufacturing process characterized by the absence of thermal energy in the shaping process. Indeed, it is a two-step process where the manufactured objects are printed and densified in separate steps. The printing step consists of high-precision ink jet printing of binder on metal powder bed substrate. Metal powder is bonded together when binder is jetted on the powder bed in a selective manner, corresponding to the cross-sectional shape of the objects being manufactured. In a cyclical way, the powder bed is lowered and recoated with additional loose powder on top to form the next layer, to which the binder is printed. This is done layer by layer until the whole build box is used and filled with metal powder. The printed objects are now located in three dimensions inside the build box, supported by loose metal powder. In this stage, the objects are in a green state (consolidated powder forms, held together by binder, that have not yet been sintered for final strength). The green objects are then cleared from powder with vacuum and compressed air in a closed environment. The green objects are then placed on ceramic plates and densified in a following sintering step. The objects shrink during the sintering. It is in this step that the metal particles fuse together, and the objects receive their strength, density, and material properties. After sintering, the objects can be subject to additional process and heat treatments as per conventionally manufactured counterparts. A schematic of the Metal Binder Jetting Process is shown in Figure 1.

Since forming, or 3D printing, and sintering are separate, Metal Binder Jetting Additive Manufacturing allows for a wide materials selection, where the process can be optimized for each material selection. Virtually, all materials that can be sintered can be processed via Metal Binder Jetting Additive Manufacturing as long as they are available in powder form with properties within the limits suitable for the printing process. Powder characteristics such as particle size, powder morphology, density, and flowability affect the printing process, therefore limiting the range of powders that can be processed.

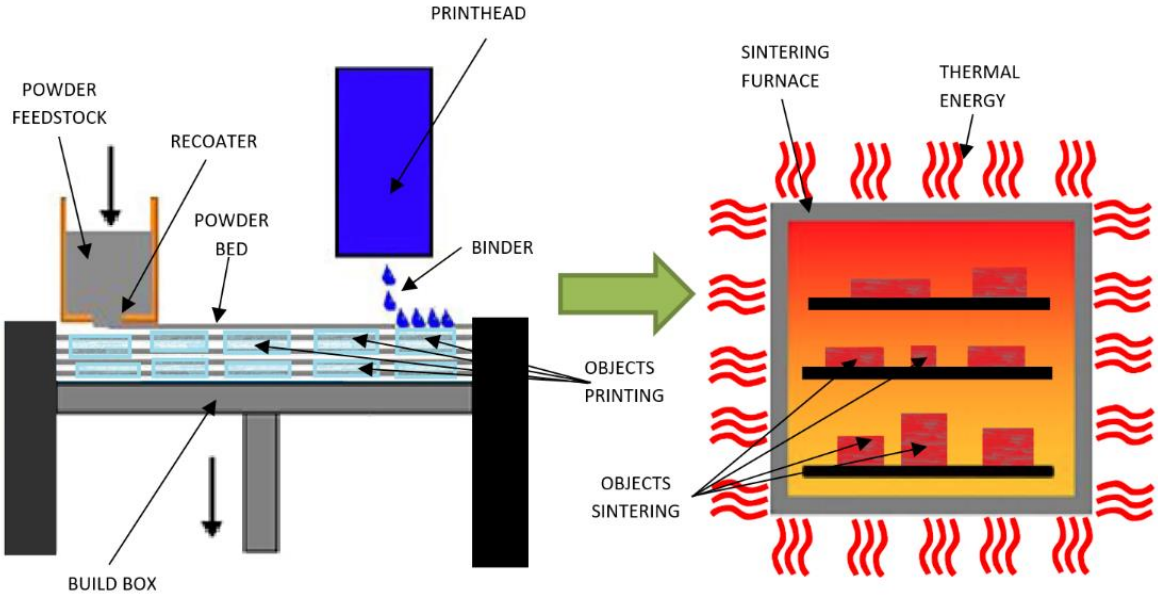


***Figure 1**. Schematic of Metal Binder Jetting Additive Manufacturing process, consisting of 3D printing at room temperature followed by sintering.*

## 1.2 Review of superalloy MAR-M-247™ conventional fabrication methods

Superalloys encompass a group of metallic alloys which are utilized structurally at operating temperatures of 538 °C (1000 °F) or higher [ [1] ]. Superalloys are referred to as "super" due to their ability to exhibit outstanding strength at temperatures as great as 85 % of their melting points (0.85 $T_M$). Such alloys consist of an austenitic face centered cubic (FCC) matrix (γ), dispersed intermetallic FCC gamma prime (γ') precipitates that are coherent with the matrix, plus carbides, borides, and other phases which are distributed throughout the matrix and along the grain boundaries. Property attainment with superalloys is principally a function of: (a) the amount and morphology of γ', (b) grain size and shape, and (c) carbide distribution [ [2] ]. Superalloys exhibit superior elevated temperature properties and are used in applications involving the highest temperatures and highest stresses. Such applications include gas turbine engine components, the subject of this project. In addition to maintaining high strength at temperatures approaching 85 % of the melting point, these materials exhibit good hot corrosion, oxidation, and sulfidation resistance required in the gas turbine environment due to the presence of the contaminants sodium, potassium, vanadium, and lead present in the intake and liquid or gas fuel [ [3] ].

Among superalloys, the alloy MAR-M-247™ (and its derivatives) boasts particularly high creep strength at high temperatures, good castability, along with excellent oxidation resistance. [ [4] ]. These are very desirable properties that make the alloy a perfect candidate for demanding applications such as aircraft engine components, industrial engine blades, vane segments, integral axial turbine wheels, fuel nozzles, and high-performance turbocharger wheels.

MAR-M-247™ is a nickel-base superalloy with a high γ' [$Ni_3$ (Al, Ti)] volume fraction (> 60 %) and high refractory element (Ta + W + Mo) content (13.7 %). The nominal composition was developed in the early 1970s by Danesi, Lund, and others at Martin Marietta Corporation (now merged in Lockheed Martin) [ [5], [6] ]. The alloy was originally developed for conventional equiaxed casting of turbine components and presents high creep strength at high temperatures and good castability, along with excellent oxidation resistance [ [7] ]. The advent and development of Directional Solidification (DS) and Single Crystal (SX) casting processes in the late 1970s engaged a fruitful material-process development period in which many MAR-M-247™ derivatives have been extensively investigated and documented in the literature [ [8] ]. Equivalent alloys designations include MM-0011 (developed by Martin Marietta Corporation), René108™ (developed by General Electric), and CM247LC™ (developed by Cannon Muskegon Corporation) [ [9] ].

However, the alloy MAR-M-247™ is considered un-weldable due to the high volume fraction of the γ′ phase and its cracking susceptibility. This relationship between the cracking susceptibility and γ′ fraction is attributed to the precipitation hardening that occurs within the aging temperature of the alloy; reheating the material to within this region results in hardening accompanied by a reduction in ductility leaving the material prone to cracking [ [10] , [11] ]. Therefore, the manufacturing process of MAR-M-247™ components has been commercially limited to casting-based processes. Moreover, MAR-M-247™ is characterized by poor machinability, which is required for the manufacturing of components since the casting process is limited to bar stock material fabrication or near-net shape with poor accuracy. In summary, the characteristics that make MAR-M-247™ a desirable alloy for demanding high temperature applications are counterbalanced by highly undesirable challenges in the manufacturing process.

For the reasons explained above, fusion-based additive manufacturing technologies such as Laser-Powder Bed Fusion, Direct Energy Deposition, and Electron Beam Melting, are not suitable to process MAR-M-247™ due to the high thermal gradients involved in the process. Despite that, Additive Manufacturing of MAR-M-247™ has been attempted by many, and numerous studies on the crack behavior have been

published, but crack-free processing has not been achieved other than by employing highly specialized equipment in research projects, nor has it been achieved commercially to the knowledge of the authors [ [12] , [13] ].

MAR-M-247™ has also been manufactured via Metal Injection Molding (MIM) Powder Metallurgy, but not without serious processing challenges. Although several successful feasibility studies have been published, the commercial application of MIM MAR-M-247™ and its derivatives is limited. The available information suggests that MIM superalloys like MAR-M-247™ have been investigated in industry but have not progressed very far in terms of application maturity. [ [14] , [15] , [16] , [17] ] The authors hypothesize that the limited application of MIM MAR-M-247™ derivatives is due to: (a) the typical market requiring medium to low production volumes, which are not cost effective for MIM due to the entry requirement of manufacturing complex molds, (b) the typical market requiring advanced material properties to which the MIM process has not been yet optimized, and (c) the typical market requiring secretive operations and therefore causing a lack of information about this topic.

### 1.3 Metal Binder Jetting of superalloy MAR-M-427™

In an attempt to develop an additive manufacturing process that would overcome the manufacturing limits of fusion-based technology, as well as the entry requirements of metal injection molding, and the manufacturing challenges of traditional casting and machining, a process was developed by Digital Metal to fabricate MAR-M-247™ objects via Metal Binder Jetting Additive Manufacturing [ [18] ]. The material-process was commercialized in 2019 with the name DM 247™ [ [19] ]. Similar efforts to develop a material-process for binder jetting of MAR-M-247™ derivative superalloys are being pursued by other additive manufacturing companies developing binder jetting equipment such as General Electric and ExOne (now Desktop Metal), but have not yet been fully commercialized [ [20] ].

Metal Binder Jetting Additive Manufacturing gained interest in recent years thanks to the high design freedom, short production lead time, and adequate production cost in certain applications. Metal Binder Jetting of superalloy MAR-M-247™ is significant because this additive manufacturing method can be used to fabricate complex geometries at high production rates and relatively low production costs. Conventional manufacturing methods for this superalloy present many challenges due to the poor weldability and machinability of the material, while Metal Binder Jetting is a promising technology since it can overcome such limitations thanks to the heatless forming process followed by uniform sintering of the fabricated parts. This study is specifically aimed to qualify superalloy MAR-M-247™ for production via Metal Binder Jetting of a turbine wheel operating at high temperatures, designed for increased efficiency compared to a nickel alloy conventionally machined from solid.

Thus, the thrust of the current program engaged by the authors and their respective companies is to demonstrate the commercial applicability of Metal Binder Jetting Additive Manufacturing as a fabrication method for superalloy objects, as well as to improve the overall manufacturing process efficiency, and ultimately optimize the alloy's high temperature mechanical properties response through optimized Hot Isostatic Pressing strategies, Solutioning, and Aging heat treatment processes. Program details, along with pertinent results follow. Note that the program is still in process and as such this writing represents an interim report.

## 2. Experimental Process & Methods

### 2.1 Material

Spherical shaped gas-atomized powder DM 247™, commercialized by Digital Metal, was used as a feedstock material in the Metal Binder Jetting process. The median particle size at 50% of the volume distribution, D50, was 15 μm. Theoretical density is 8.54 g/cm$^3$. The chemical composition was determined by Inductively Coupled Plasma Mass Spectroscopy (ICP-MS), and it is within the composition specifications of the original formulation of the superalloy MAR-M-247™ by Martin Marietta corporation, as shown in Table 1 [ [4] , [21] ]. The name DM 247™ is used by Digital Metal to differentiate the alloy as a proprietary Metal Binder Jetting version, and for trade marketing reasons.

The binder material used for forming the green component is C20, a water-based organic binder with composition proprietary to Digital Metal, who commercializes it.

***Table 1.*** *Chemical composition (%, typical values) of DM 247™ and MAR-M-247™ original composition*

| | Al | B | C | Co | Cr | Hf | Mo | Ni | Ta | Ti | W | Zr | Nb | V |
|---|---|---|---|---|---|---|---|---|---|---|---|---|---|---|
| **MAR-M-247 (original formulation)** | 4.5 - 6.7 | .002 - 0.2 | 0.04 - 0.35 | 7 - 13 | 7 - 13 | 0.7 - 5 | < 0.7 | Bal. | < 5.0 | 0.6 - 5.0 | < 14 | < 0.15 | < 2.2 | < 1.1 |
| **DM 247 (Digital Metal)** | 5.4 | .012 | 0.13 | 9.9 | 8.3 | 1.3 | 0.66 | Bal. | 3.0 | 1.0 | 9.8 | 0.05 | - | - |

### 2.2. Printing

The turbine wheel component was designed by the end user, and the test specimens were designed in accordance with the ISO 2740 standard. The designs were transferred in CAD format to the print preparation software, in which all printed components were rescaled with a volumetric scaling factor of 1.71 prior to printing to account for the subsequent shrinkage during sintering. Subsequently, the models were arranged in 3D space corresponding to the build box and then sliced in two-dimensional files corresponding to the cross-sections of the build at 42 μm thickness. Preparation of the print job, also known as slicing, was performed using the software Materialize Magics. Printing parameters were set using the Digital Metal Build Preparation software. Layer height was set at 42 μm, binder-powder saturation at 69 % with a printing speed correspondent to 100 cm$^3$/hr. Overall, the parameters used did not deviate significantly from the printing parameters typically used on the Digital Metal machines, which were previously developed and optimized for other materials. Forming of the green components was performed via Metal Binder Jetting Additive Manufacturing, or 3D printing, in a Digital Metal DM P2500 printer. Both the turbine wheel components and the specimens designed were printed within the same print build and with the same exact material and parameters settings.

After the printing was completed, the entire build box was cured at 200 °C (392 °F) in air atmosphere to evaporate the solvent present in the ink and crosslink the binder, to strengthen the powder-binder compound enough to be handled in the green state. Subsequently, the entire build box was placed inside a manual de-powdering cabinet, where all the loose powder was removed from the printed components and collected to enable the reuse of the powder in future print jobs.

## 2.3 Debinding and Sintering

After the printed objects were removed from the de-powdering cabinet, they were staged on ceramic plates in preparation for the subsequent sintering process. Prior to sintering, the parts were debinded in air atmosphere at 345 °C (653 °F) for 3 hours to break and partially evacuate the binder used in the 3D printing process for shaping. Sintering was performed in a Nabetherm VTH40-Mo in 50 mBar (37 Torr) partial pressure Argon atmosphere at 1315 °C (2400 °F) for 4 hours.

## 2.4 Hot Isostatic Pressing and Post Heat Treatments

After sintering, the manufactured objects were subjected to Hot Isostatic Pressing to further consolidate the structure and eliminate the residual porosity. Thereafter, they were subjected to post heat treatments, to alter the microstructure and give the alloy the desired material properties.

The post-processing was split into three separate paths, to assess differences in process efficiency and the resulting material properties:

a) *HIP-Sol-Age1000-Age800* - conventional HIP followed by conventional solution heat treatment, followed by a long double aging.
b) *HPHT-Age1000-Age800* - A HPHT™ cycle combining HIP and solution heat treatment in the HIP vessel, followed by the same double aging as for the previous trial.
c) *HPHT-Age870* - A HPHT™ cycle combining HIP and solution heat treatment in the HIP vessel, followed by a short single aging.

**- HIP-Sol-Age1000-Age800:** The first post-processing path was aimed to reproduce and follow the process typically utilized in industry and reported in the literature. Conventional HIP was performed in a Quintus QIH15L press furnace at 1185 °C (2165 °F) for 4 hours with a pressure of 150 MPa (21.8 ksi) applied via high purity Argon gas, followed by natural furnace cooling before reclaiming the process gas. Subsequently, a solution heat treatment was performed in a conventional industrial-type heat-treatment vacuum furnace at 1260 °C (2300 °F) in an Argon atmosphere for 4 hours, then cooled via forced gas cooling at 1.22 Bar (17.7 psi) Argon. The median cooling rate achieved was ~ 127 °C/min (260 °F/min) down to 926 °C (1700 °F), and ~ 80 °C/min (176 °F/min) down to 300 °C (572 °F). Finally, aging heat treatment was performed in an Elnik3015 furnace in Argon atmosphere, first for 10 hours at 1000 °C (1832 °F), and subsequently for 20 hours at 800 °C (1472 °F), with natural furnace cooling.

**- HPHT-Age1000-Age800:** The second post-processing path was aimed to improve process efficiency by combining HIP and Solution heat treatment into a single process step within the HIP vessel. This combined process step is referred to as High Pressure Heat Treatment (HPHT™), and is made possible by the proprietary Uniform Rapid Cooling (URC®) and Uniform Rapid Quenching (URQ®) processes developed by Quintus and featured in their modern production furnaces [ [22] ]. URC® increases the natural cooling speed by up to a factor of 10-15 over conventional systems, while stirring the gas so the cooling is more uniform in the hot zone. This can be achieved with fans or ejectors and Quintus delivers both techniques with the option of controlled cooling. URQ® is very fast cooling at a rate above 200 °C/min (392 °F/min) gas rate with cycle load down to 600 °C (1112 °F), allowing quenching of most materials at the same or higher rate as commercial oil quench equipment. An additional benefit of the highly pressurized gas involved in the cooling segment is that it produces an entire production load that

will receive more or less the same cooling rates. Originally introduced for productivity improvement, these technologies now offer the cooling rates, accuracy, and uniformity to perform many of these post processing steps all in a HIP vessel. For this investigation the HPHT™ was performed in a Quintus compact press furnace at 1260 °C (2300°F) for 4 hours with a pressure of 150 MPa (21.8 ksi) applied via high purity Argon gas, followed by Uniform Rapid Cooling (URC®) at a rate up to 250 °C/min (450 °F/min) to below 500 °C (932 °F). After the combined HIP and solution heat treatment, aging was performed in the same way as in the previous trial, in an Elnik3015 furnace in argon atmosphere, first for 10 hours at 1000 °C (1832 °F), and subsequently for 20 hours at 800 °C (1472 °F), with natural furnace cooling.

- **HPHT-Age870:** The final path was aimed at further improving both the final microstructure, as well as the process efficiency, by simplifying and shortening the aging treatment. The HPHT™ step was again performed in a Quintus press furnace at 1260 °C (2300 °F) for 4 hours, with a pressure of 150 MPa (21.8 ksi) applied via high purity Argon gas, followed by Uniform Rapid Cooling (URC®) at a rate up to 250 °C/min (450 °F/min) to below 500 °C (932 °F). Thereafter, aging was performed in an Elnik3015 furnace in an Argon atmosphere at 870 °C (1600 °F) for 8 hours. The 1000 °C (1832 °F) step was eliminated both to improve process efficiency and also to decrease the formation of grain boundary carbides, in the hopes of improving ductility.

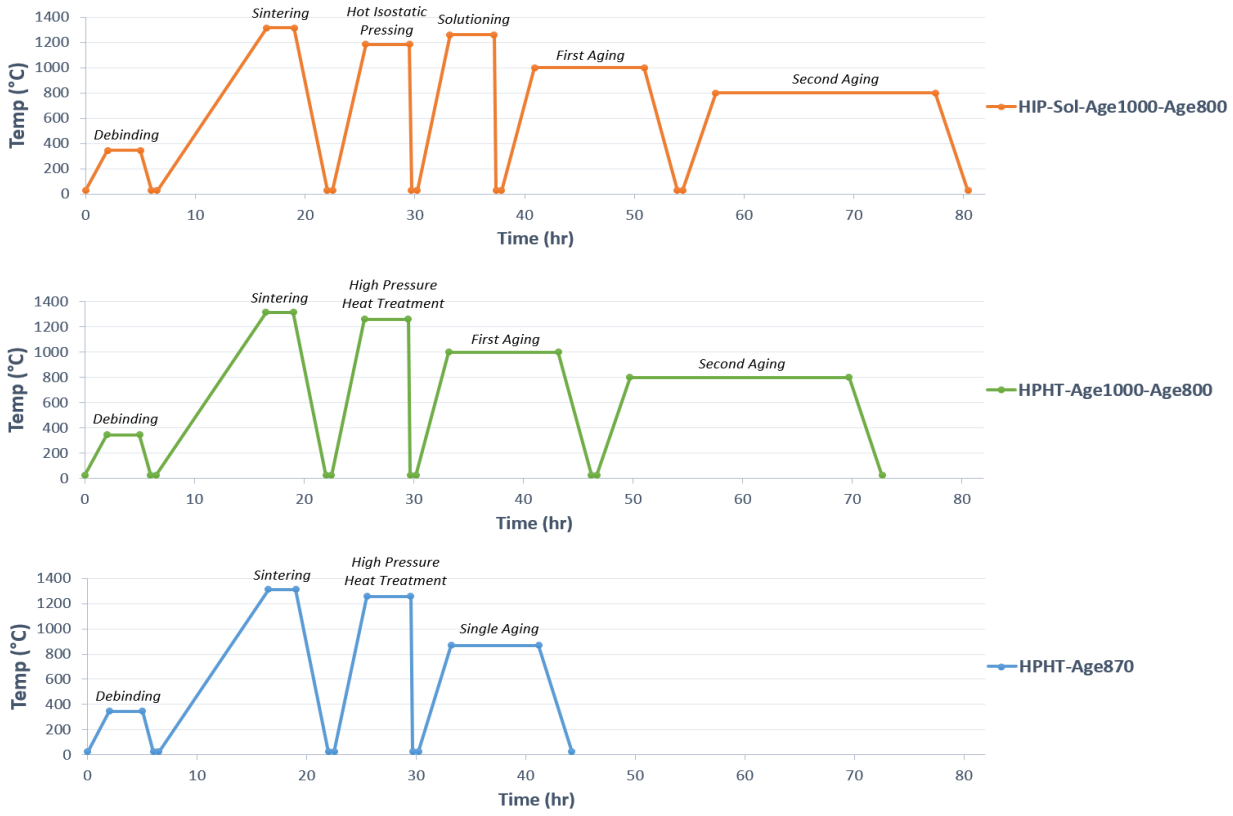


***Figure 2.*** *Simplified time-temperature graph of the process for the three conditions investigated.*

## 3. Results

### 3.1 Microstructure

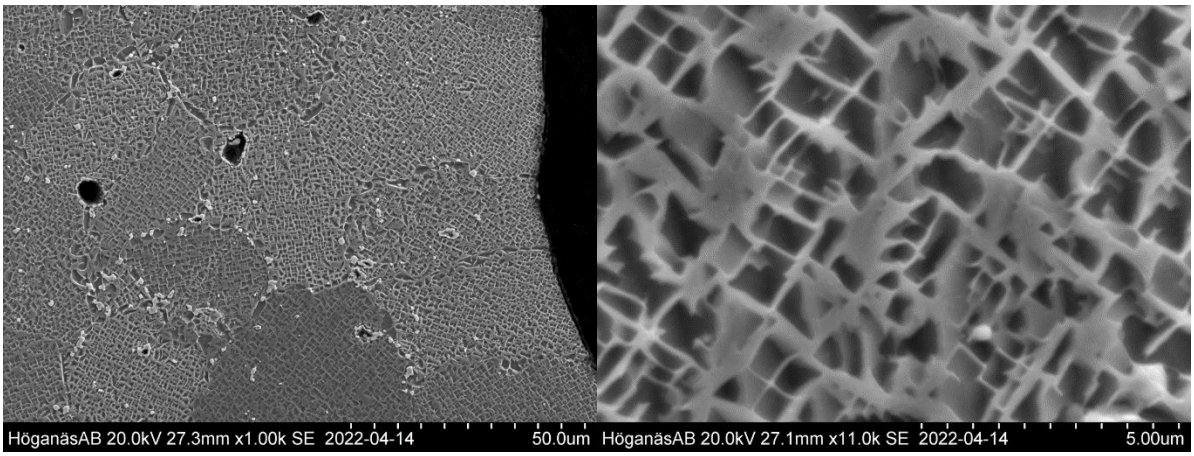


***Figure 3.*** *In-process microstructure (two magnification levels), after* ***sintering***

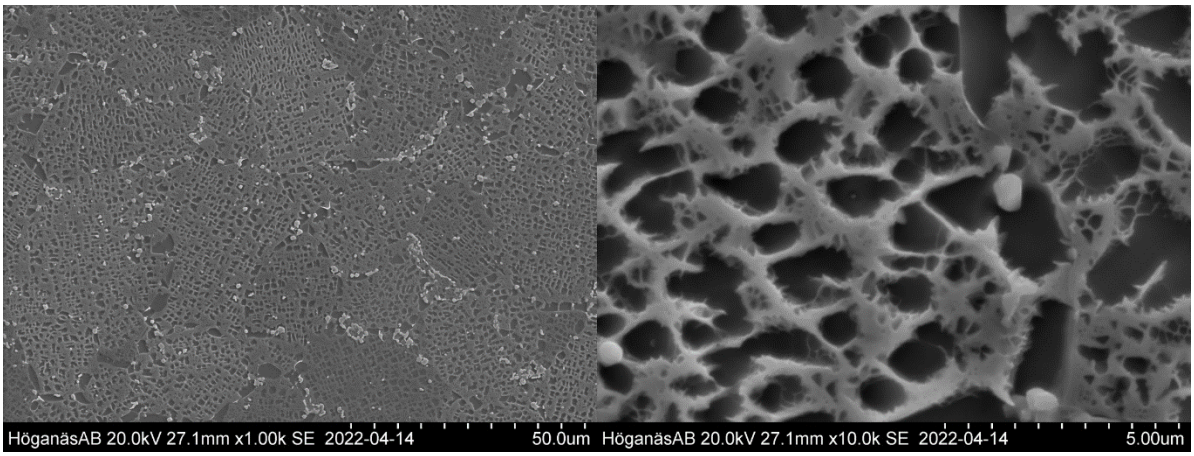


***Figure 4.*** *In-process microstructure (two magnification levels), after* ***Hot Isostatic Pressing***

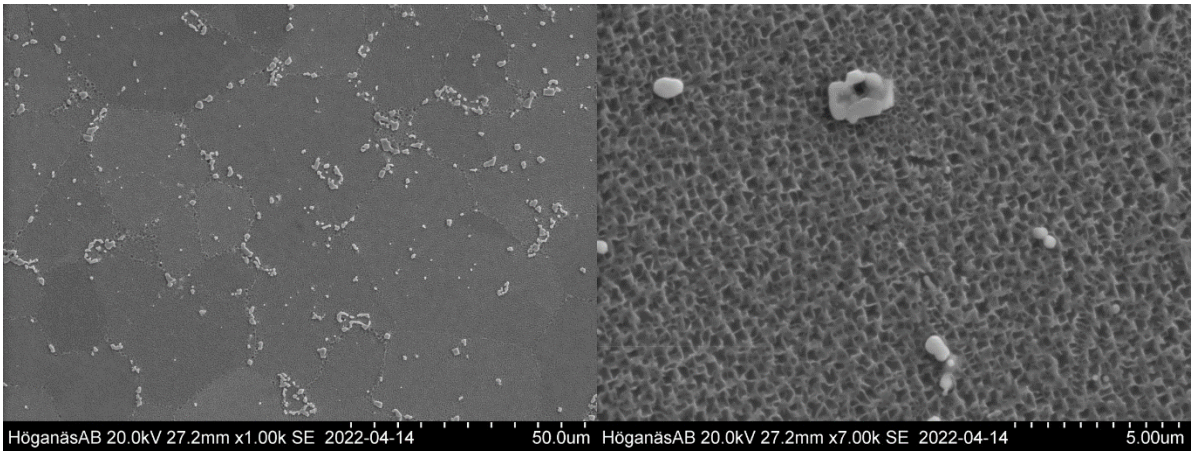


***Figure 5.*** *In-process microstructure (two magnification levels), after* ***High Pressure Heat Treatment***

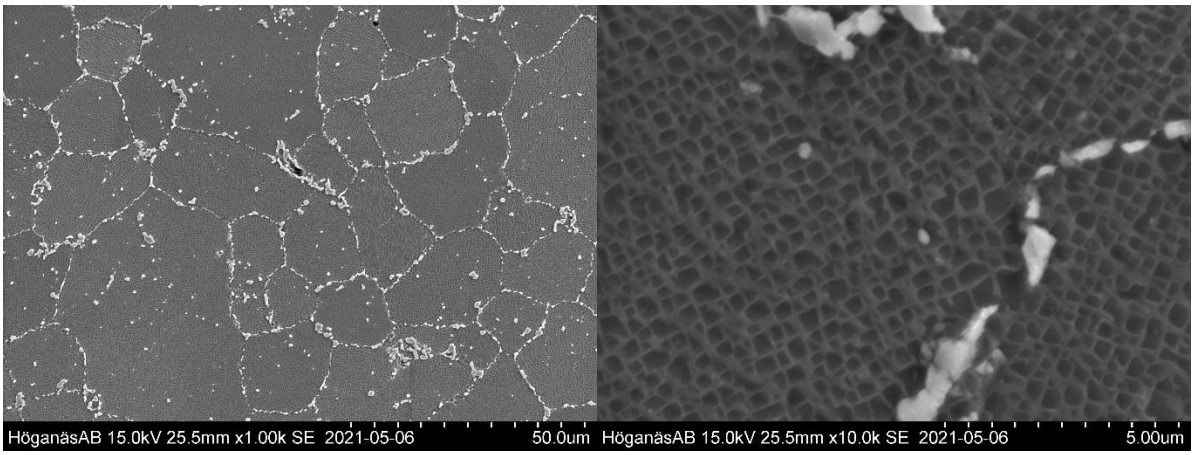


***Figure 6.*** *Final microstructure (two magnification levels),* ***HIP-Sol-Age1000-Age800***

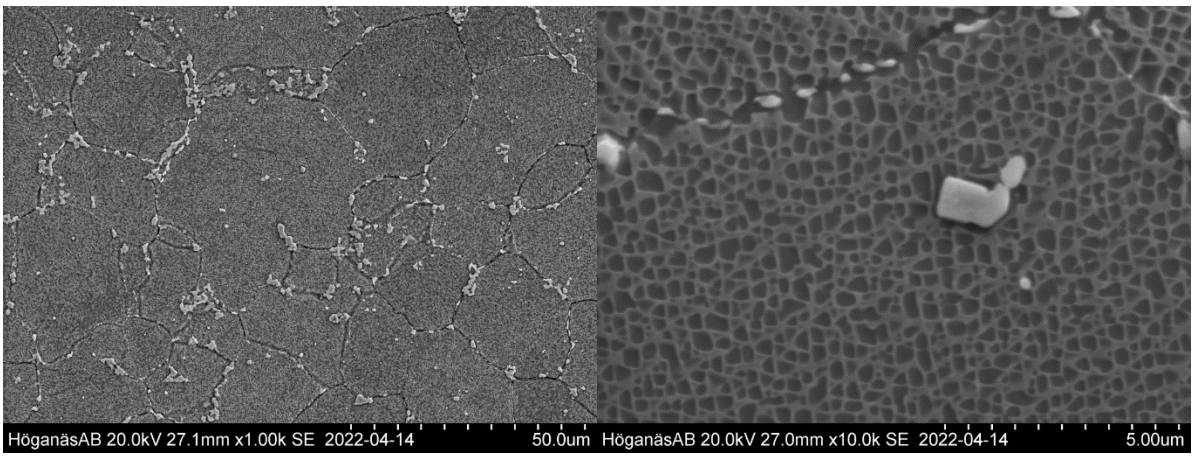


***Figure 7.*** *Final microstructure (two magnification levels),* ***HPHT-Age1000-Age800***

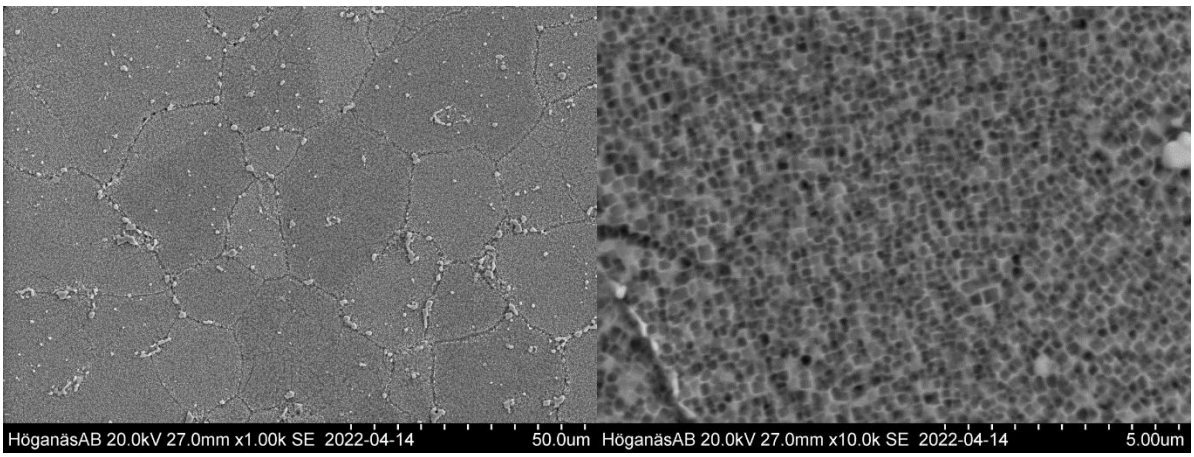


***Figure 8.*** *Final microstructure (two magnification levels),* ***HPHT-Age870***

## 3.2 Tensile testing at room temperature

Tensile testing at room temperature has been performed as a relative metric, to assess the performance at various stages throughout the process, and to compare the different heat treatments. The intended use of the alloy is at elevated temperatures, thus rendering the room temperature properties to be of less importance.

***Table 2.*** *Tensile testing at room temperature for multiple process conditions. "Sintered" "HIP" and "HPHT" tests were performed for mid-process evaluation.*

| Specimen Process Condition | Count | Elastic Modulus | | Yield Strength | | Ultimate Tensile Strength | | Elongation |
|---|---|---|---|---|---|---|---|---|
| | | GPa | 10^6 psi | MPa | 10^3 psi | MPa | 10^3 psi | % |
| *Sintered* | 13 | 213 | 30.9 | 793 | 115 | 1289 | 187 | 20.9 |
| *HIP* | 1 | 199 | 28.9 | 785 | 114 | 1300 | 189 | 17.5 |
| *HPHT* | 1 | 208 | 30.1 | 1026 | 149 | 1311 | 190 | 11.6 |
| *HIP-Sol-Age1000-Age800* | 6 | 204 | 29.6 | 1052 | 153 | 1228 | 178 | 7.2 |
| *HPHT-Age1000-Age800* | 5 | 213 | 30.9 | 1084 | 157 | 1316 | 191 | 9.5 |
| *HPHT-Age870* | 5 | 216 | 31.3 | 1077 | 156 | 1391 | 208 | 12.9 |

## 3.2 Tensile testing at high temperature

Tensile testing at high temperatures has previously been performed on samples of this alloy DM 247™ made through Metal Binder Jetting. Similar processing conditions as those used in *HIP-Sol-Age1000-Age800* route presented in this paper were used for sintering, HIP, solutioning, and aging heat treatments, although not identical. Testing of the current process conditions is intended, though not yet completed.

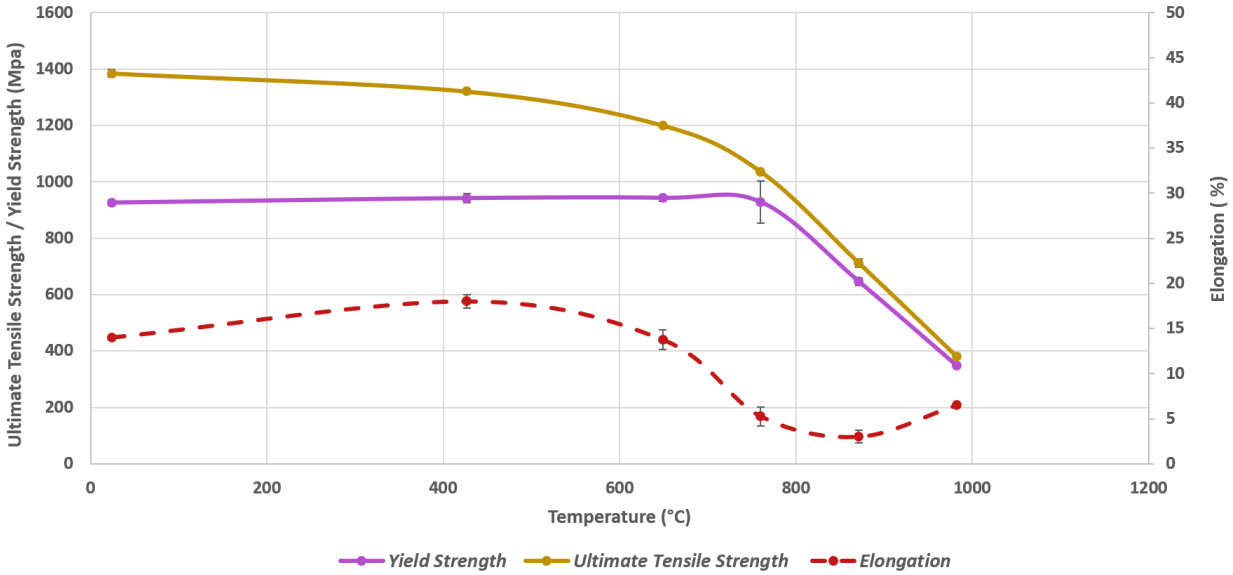


***Figure 9.*** *Tensile testing of DM 247™, performed at several different temperatures. Processing condition tested were similar those used in the* ***HIP-Sol-Age1000-Age800*** *route presented in this paper.*

## 3.2 Stress rupture

The reason for using this superalloy is its ability to withstand stress at high temperatures. In fact, the whole meaning of this project is centered on the fact that this alloy can be used at higher temperatures over alternative superalloys currently being produced via additive manufacturing. Therefore, the authors consider high-temperature creep rupture testing as a valid metric to measure the performance of this alloy in its intended high-temperature applications. If the intended use was not such high temperature, there are other metal alloys with better performance at lower temperatures and better manufacturing economics.

The end user communicated an indicative target that was originally intended for cast directionally solidified MAR-M-247™. The authors used that target as a reference, acknowledging that the polycrystalline alloy manufactured via Metal Binder Jetting may not be able to compete in performance with the directionally solidified version of the same alloy.

For the scope of this study, the creep rupture performance has been measured at the temperatures suggested by the target, and the results are used as the main metric of evaluation.

***Table 3****. Stress rupture testing results (HIP = conventional Hot Isostatic Pressing, HPHT = combined High Pressure Heat Treatment)*

| **Heat treatment type**<br>**Aging treatment, Temp(C)Time(Hr)** | **Standard HIP & Solution + 1000C10HR +800C20HR** | | **Combined HPHT + 1000C10HR +800C20HR** | | **Combined HPHT + 870C8HR** | | **Target** | |
|---|---|---|---|---|---|---|---|---|
| Test temperature (C) | 760 | 982 | 760 | 982 | 760 | 982 | *760* | *982* |
| Stress, initial (KSI) | 90 | 30 | 90 | 30 | 90 | 30 | *90* | *30* |
| Life Hours @ 30 KSI | - | 4.5 | - | 5.9 | - | 5.4 | - | - |
| Life Hours @ 90 KSI | 25.1 | - | 26.3 | - | 26.9 | - | - | - |
| Life Hours @ 100 KSI | 12.8 | - | 8.0 | - | 5.9 | - | - | - |
| Life Hours (total) | **37.9** | **4.5** | **34.3** | **5.9** | **32.8** | **5.4** | ***25.0*** | ***25.0*** |
| % Elongation | 1.0 | 4.0 | 1.5 | 5.3 | 3.2 | 2.5 | *1.0* | *6.0* |
| % Reduction Area | 1.3 | 0.6 | 3 | 2.3 | 2.3 | 1.4 | *2.0* | *6.0* |

## 3.3 Application and In-field Testing

The application is a high temperature turbine wheel, designed for increased efficiency compared to a conventional nickel alloy machined from solid. Due to the manufacturing challenges of MAR-M-247™ via conventional methods, it is often avoided. The less-ideal but more manufacturable material IN718 is therefore chosen for the application, mandating a lower operating temperature.

Based on design data from the end user, the use of Metal Binder Jetting Additive Manufacturing DM 247™ results in 5+% increased total efficiency gain vs. the conventional nickel alloy machined from solid due to high temperature survivability. The efficiency gain is largely a function of getting away from IN718 and getting to a higher operating temperature.

The efficiency gain is especially important for those applications where the overall system weight is critical for the application. Therefore, the total amount of fuel carried can be minimized by a maximized system efficiency, which is given by the higher operating temperature.

Moreover, the end user claims an over 40% cost reduction by using Metal Binder Jetting Additive Manufacturing, largely due to the production volumes. Conventional methods would start with the casting of the raw material, followed by machining from stock. The casting operation would have required tooling, which is not cost effective for low volumes, and a long lead time since this is a relatively rare alloy (as now, the availability of specialized foundries to cast-to-order is typically several months out). Indeed, the end-user claims an over 70% reduction in lead time reduction compared to conventional methods.

***Table 4.*** *Comparison of key metrics between conventional manufacturing process and Metal Binder Jetting Additive Manufacturing.*

| Metric | Conventional Process (Casting + stock machining) | Metal Binder Jetting Additive Manufacturing + finish machining |
|---|---|---|
| Application Efficiency | Ref. | +5% |
| Manufacturing Cost | Ref. | - 40% |
| Lead Time | Ref. | - 70% |

The following manufacturing steps, not covered in this paper, include finish machining, inspection, balancing and functional measuring. Subsequent field testing consists of high temperature overspeed spinning.

The exact application and related data, such as rotational speed and service temperature, are not disclosed since they are proprietary information to the end-user.

## 4. Discussion

The etched microstructures look rather similar for the different processes when viewed from afar; textures inside the grains, similar grain sizes, and with carbides and oxides decorating the grain boundaries. The main thing standing out is the visible pores in the as-sintered material, which is expected for a material made from powder.

When comparing the finer structures, however, there is a clear difference between various processes. The as-sintered and the as-HIP samples have a coarser γ-γ' structure compared to the rest, with varying degrees of organic-looking and geometrically shaped structures in different regions. This is likely due to the relatively slow cooling rate at the end of the sintering and HIP cycles, allowing for extensive precipitation of γ’ to occur, rather uncontrollably, during cooling.

All the heat treatments lead to considerably more homogenous and finer γ-γ' textures, attributed to the high cooling rates after the solutioning and the HPHT™ steps respectively. The double aging heat treatments yield very comparable microstructures for the conventional HIP + solutioning samples and the combined HPHT™ samples. However, there is a noticeable difference between the two methods in the size, amount, and distribution of grain boundary carbides present. Perhaps, the different grain boundaries resulting from different process conditions could be used as a gauge to control certain behaviors.

The shorter single step aging, performed at 870 °C (1600 °F), results in an even finer and more homogenous γ-γ' structure, and a reduction in grain boundary carbides, as originally intended.

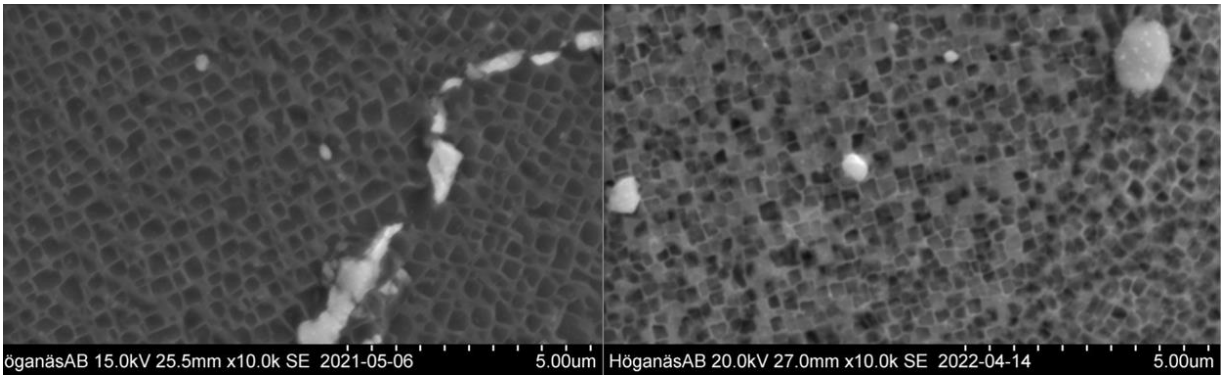


***Figure 10:*** *Left: Conventional "HIP-Solution-Age1000C-Age800C"; Right: combined "HPHT-Age870C". Note the smaller gamma prime size in the right image. Note the "empty" spots between gamma prime squares in the right image.*

There seem to be some γ' precipitates "missing" in the structure from the single step aging. Two step age could contribute to forming a bimodal distribution of gamma prime strengthening phase, which seems to be lacking in the single step age. However, it would require much higher magnifications to capture this phenomenon. It is difficult to tell whether this comes from the structure being insufficiently aged, which would be a reasonable assumption, or alternatively, whether the finer structure is more difficult to reveal through etching. The very thin γ sections are also being etched away, albeit at a slower rate than the γ' precipitates. Either way, it is difficult to accurately determine the γ/γ' ratio in this case. If the structure is indeed underaged, an approach to resolve this would be to increase the aging time or to add a second step at a lower temperature, at the expense of process efficiency.

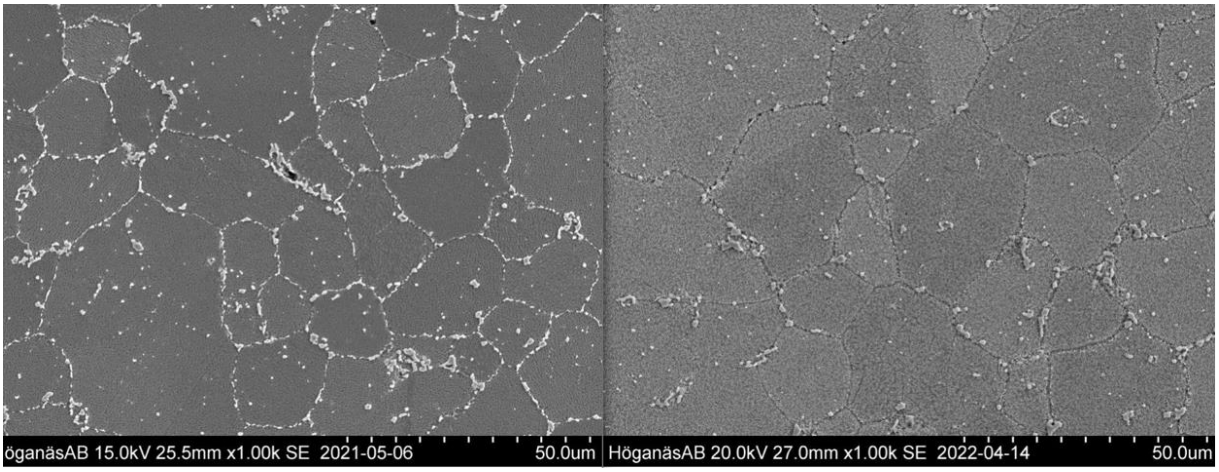


***Figure 11:*** *Left: Conventional "HIP-Sol-Age1000C-Age800C"; Right: combined "HPHT-Age870C". There is a considerable difference between the processes in the amount of carbides present at the grain boundaries. However, also note that the effect has been (unintentionally) strengthened visually by the differences in contrast and settings used during imaging.*

Comparing the double aging and the single step aging, the results are overall rather similar, suggesting that 30 hour long aging treatments might be unnecessary. The HPHT™ process results in noticeably fewer grain boundary carbides formed, compared to the conventional HIP + solutioning, the reason for

which has not been fully determined. Furthermore, the single step aging provides even fewer grain boundary carbides, while further refining the γ-γ' structure.

The advantages of these effects can be seen in the room temperature tensile tests, as the strength and the ductility increase with these more efficient processes, when compared to the more conventional process. The HIP does not seem to improve the properties of the material itself since the material is already at a very high density right after sintering. The negative effects of the pores are likely masked by the high ductility that the material exhibits in the as-sintered and non-hardened state, allowing the material to release stresses by deforming, without initiating and propagating cracks around any weak points. However, dynamic properties such as fatigue would seek out these weak points showing a negative impact on the non-HIP condition. The negative effects would probably be much more severe when the material has been hardened, therefore still rendering HIP or HPHT™ necessary for a high-performance material.

Overall, the stress rupture tests showed satisfactory results at 760 °C (1400 °F) but fell far short of the target at the 982 °C (1800 °F) testing condition. Combined HPHT™ routes performed similarly or slightly under the conventional HIP route for 760 °C (1400 °F), but outperformed the conventional HIP route at elevated temperature testing at 982 °C (1800 °F). Although grain boundary carbides might have a negative impact on the ductility of the material at the lower temperatures, they can potentially be beneficial at higher temperatures by hindering grain boundary sliding. They can improve the creep resistance of the material in temperature regions where the creep is dominated by grain-boundary-related phenomena [ [23] ]. However, since the stress rupture performance is lacking at the highest temperatures, despite having a highly refined γ-γ' microstructure, combined with an abundance of grain boundary carbides in some of the cases, this suggests that some other aspect needs to be addressed to further improve the high temperature performance. The authors suspect that the creep at the higher testing temperature happens mainly due to intergranular phenomena, which are exaggerated by the small grain sizes. If so, one approach would be to promote grain growth, although that might be difficult due to the abundance of carbides pinning the grain boundaries. In detail, since the Metal Binder Jetting alloy is made from powder particles, the particle boundaries get pinned in what will become grain boundaries by carbides, which are present in the master alloy but also may be added in the form of additional carbon left behind from the binder employed in the printing process if not carefully evacuated in the debinding process. Moreover, it is desirable to increase the grain size to increase ductility. Using a low-carbon derivative of the alloy, such as CM247LC™ (developed by Canon-Muskegon Corporation), and implementing a grain coarsening step at 1290 °C (2354 °F) for 20 hours, has shown to generate considerably larger grain sizes and thus increase the creep resistance of a material produced by Metal Injection Molding [ [24] ]. Differential Thermal Analysis has determined empirically the γ' solvus temperature to be 1246 °C (2275 °F) for a superalloy composition with an Aluminum + Titanium content of 6.5 % (corresponding to ~ MAR-M-247™), therefore it is hypothesized that a prolonged hold at a temperature slightly above the γ' solvus temperature would result in grain coarsening [ [25] ]. It is also hypothesized that a longer sintering time could initiate grain growth behind the original powder particle boundaries, although a much longer sintering time would require a slightly lower sintering temperature to avoid deformation of the printed object. The authors plan to verify these effects experimentally on material produced by Metal Binder Jetting.

Regarding the elongation and reduction in area results, it appears that some measuring discrepancies are present. The Reduction Area (RA) should always be equal to or greater than the elongation because of conservation of mass and any specimen necking during tensile testing. In one of the readings, elongation

is 4 % and but the Reduction Area is 0.6 %, which seems incongruent. Due to the small size of the specimens, the authors hypothesized that there is a measuring error and plan to repeat the testing.

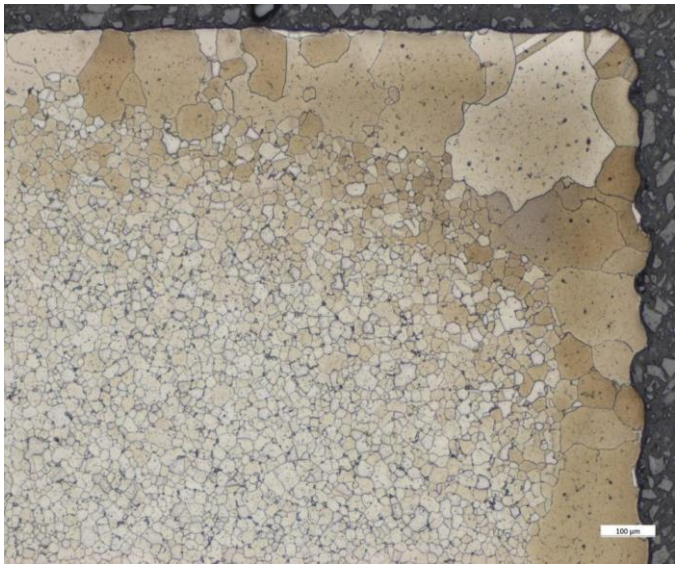

***Figure 12.*** *Process condition 21 conventional "H.I.P.-H.T-+Age1000-Age800" LOM etched moclonics*

***Figure 13.*** *Process condition "HPHT+Age1000+Age800" LOM etched moclonics.*

Light decarburization is observed on the outer layer of most specimens up to a depth of 50-100 um. Such decarburization in the outer layer leads to grain growth which is facilitated by the lessened amount of carbides pinning the grain boundaries in this area. This phenomenon is much more pronounced in the conventional process condition with separated HIP and solutioning than in the HPHT™ process, where the two steps are combined. The reason for this difference is not fully understood, but it suggests that the main contributor to the outer layer decarburization and grain growth is in fact the separate solutioning treatment. Although the recorded dewpoint of argon was less than -51 °C (-60 °F) with a purity of 99.998 %, the results show that the elimination of this process limited the decarburization of the outer layer. Thus, this further indicates the potential benefit of using a low-carbon version, to unpin the grain boundaries and promote grain growth throughout the material.

## 5. Conclusion

Using Metal Binder Jetting to produce MAR-M-247™ parts for turbocharger applications shows promising results. There are several benefits to be gained from additively manufacturing such parts, mainly in terms of cost and lead times, at least for certain volumes, as well as some potential performance improvements.

The High Pressure Heat Treatment (HPHT™) used in this paper allows for more efficient post processing of the material, saving time and money by minimizing the time required in some of the more complex processing equipment needed. Furthermore, it improves the properties and performance of the material in several aspects.

The simplified single step aging provides a more efficient process and better performance at lower temperatures, compared to the more conventional double aging steps. In fact, all the processes used in this paper provide excellent performance at lower temperatures and satisfactory performance when tested at 760 °C (1400 °F). However, none of them perform well enough at the highest temperatures tested, 982 °C (1800 °F), to compete with directionally solidified or single crystal material of the same alloy. It might be possible to address this issue by increasing the grain sizes in the material, though that remains to be determined.

The authors hope that the sharing of this information with others in the superalloy, powder metallurgy, and additive manufacturing community may help to further advance the state of the art of metallurgy and manufacturing process of superalloys for high-temperature applications in the transportation, energy, and industrial sectors.


***Figure 14**. Sample components printed in DM 247™ by Digital Metal*

## Nomenclature

MBJ - Metal Binder Jetting
AM - Additive Manufacturing
MIM – Metal Injection Molding
HIP - Hot Isostatic Pressing
HPHT™ – High Pressure Heat Treatment, registered trademark of Quintus Technologies
γ - gamma phase
γ' - gamma prime phase
URC® - Uniform Rapid Cooling, registered trademark of Quintus Technologies
URQ® - Uniform Rapid Quenching, registered trademark of Quintus Technologies
MAR-M-247™ - superalloy name, registered trademark of Martin Marietta Corporation
DM 247™ - superalloy name, registered trademark of Digital Metal

## Declaration of Competing Interest

The authors declare that they have no known competing financial interests or personal relationships that could have appeared to influence the work reported in this paper.

## Authorship contribution statement

**Mattia Forgiarini:** Conceptualization, Methodology, Validation, Testing, Formal Analysis, Investigation, Writing - original draft, Writing - review & editing, Visualization, Project administration. **Fredrik Berg Lissel:** Conceptualization, Methodology, Validation, Testing, Formal analysis, Investigation, Writing - original draft, Writing - review & editing. **Chad Beamer:** Conceptualization, Methodology, Validation, Formal analysis, Investigation, Writing - review & editing. **Tim Noronha:** Conceptualization, Methodology, Validation, Testing, Funding acquisition. **David Sponseller:** Methodology, Formal analysis, Investigation.

## Acknowledgments

The authors acknowledge Mats Persson of Digital Metal (Höganäs, Sweden) for the collaborative work, specifically on the sintering.

The authors acknowledge Marco Ravanal of Quintus Technologies AB (Västerås, Sweden) for the collaborative work, specifically on Hot Isostatic Pressing.

The authors acknowledge John Bressoud of Turbocam Inc (Barrington NH, United States) for the collaborative work, specifically on the creep-rupture testing.

The authors acknowledge Anna Lindström of Höganäs AB (Höganäs, Sweden) corporation for providing metallography laboratory support.

The authors acknowledge their respective companies - Azoth, Digital Metal, Quintus Technologies, Turbocam, and OMNI Metals Lab - for financially supporting this work.

## References


[1] J.B. Wahl, K Harris, “Advanced Ni-Base Superalloys for Small Gas Turbines”, The Canadian Journal of Metallurgy and Materials Science, Volume 50, Issue 3, 2011

[2] G. L. Erickson, K. Harris, R. E. Schwer, “Directionally Solidified DS CM 247 LC Optimized Mechanical Properties Resulting from Extensive y' Solutioning”, ASME 1985 International Gas Turbine Conference and Exhibit, 1985

[3] J.B. Wahl, K. Harris, “Superalloys in industrial gas turbines - an overview”, Proceedings to 9th World Conference on Investment Casting, 1996

[4] G.L. Erickson, K. Harris, R.E. Schwer, “DS CM 247 LC - enhanced mechanical properties response through optimized solutioning technique”, Paper selection of 1984 TMS-AIME fall meeting conference, Metallurgical Society of AIME, 1984.

[5] W Danesi, R Thielman, “Nickel base alloy”, Martin Marietta Corporation, United States Patent Office Ser. No. 3,720,509, 1971

[6] Carl H. Lund, John Hockin, Michael J. Woulds, “High temperature castable alloys and castings”, Martin Marietta Corporation, United States Patent Office Ser. No. 3,677,747. 1972

[7] K. Harris, G.L. Erickson, R.E. Schwer, “MAR M 247 Derivations – CM 247 LC DS Alloy, CMSX SC Alloys, Properties and Performance” Superalloys 1984: proceedings of the Fifth International Symposium on Superalloys, Metallurgical Society of AIME, 1984

[8] K. Harris, G.L. Erickson, R.E. Schwer, “Directionally Solidified and Single-Crystal Superalloys”, ASM Metals Handbook Tenth edition, Volume 1, 1990

[9] G.L. Erickson, “Polycrystalline Cast Superalloys”, ASM Metals Handbook Tenth edition, Volume 1, 1990

[10] M. J. Donachie, S. J. Donachie “Superalloys: A Technical Guide, 2nd Edition”, ASM International, 2020

[11] L. Carter, M. Attallah, R. Reed, “Laser Powder Bed Fabrication of Nickel-Base Superalloys: Influence of Parameters; Characterization, Quantification and Mitigation of Cracking”, Superalloys 2012: proceeding of the 12th International Symposium on Superalloys, the Minerals, Metals & Materials Society, 2012

[12] O. Adegoke, “Processability of Laser Powder Bed Fusion of Alloy 247LC - Influence of process parameters on microstructure and defects”, University West Licentiate Thesis, 2020

[13] T. Dahmen, N.G. Henriksen, K.V. Dahl, A. Lapina, D.B. Pedersen, J.H. Hattel, T.L. Christiansen, M.A.J. Somers, “Densification, microstructure, and mechanical properties of heat-treated MAR-M247 fabricated by Binder Jetting”, Additive Manufacturing, Volume 39, 2021

[14] B. Julien, M. Després, "Metal Injection Moulding: A Near Net Shape Fabrication Method for the Manufacture of Turbine Engine Component", Cost Effective Manufacture via Net-Shape Processing, Meeting Proceedings, 2006

[15] A. Meyer, E. Daenicke, K. Horke, M. Moor, S. Müller, I. Langer, R. F. Singer, “Metal Injection Moulding of Nickel-Based Superalloy CM247LC”, Europm2015 conference proceedings, 2015

[16] A. Meyer, R F. Singer, “Metal Injection Molding of Nickel-Base Superalloy CM247LC: Influence of Heat Treatment on the Microstructure and Mechanical Properties”, PowderMet 2017 conference proceedings, 2017

[17] B. Klöden, T. Weissgärber, B. Kieback, I. Langer, “The processing and properties of Metal Injection Moulded Superalloys”, Powder Injection Moulding International, Volume 7, No 1, 2013

[18] M. Persson, K. Glad, F. Berg Lissel “Metal Binder Jetting of Non-Weldable and Weldable Super Alloy Process and Resulting Properties”, Proceeding to EuroPM 2019 conference, 2019

[19] Digital Metal, “Digital Metal launches two superalloys for extreme applications”, digitalmetal.tech, 2019

[20] E. Martin, A. Natarajan, S. Kottilingam, R. Batmaz, “Binder jetting of Hard-to-Weld high gamma prime nickel-based superalloy RENE’ 108”, Additive Manufacturing, Volume 39, 2021

[21] Digital Metal, “DM247 Material Data Sheet”, digitalmetal.tech, 2022

[22] Quintus Technologies, “Uniform Rapid Quenching”, quintustechnologies.com, 2022

[23] F. T. Furillo, J. M. Davidson, J. K. Tien, L. A. Jackman, "The effects of grain boundary carbides on the creep and back stress of a nickel-base superalloy", Materials Science and Engineering, Volume 39, Issue 2, 1979

[24] Donald Heaney, “Handbook of Metal Injection Molding”, 2nd edition, 2019

[25] David Sponseller, "Differential Thermal Analysis of Nickel-Base Superalloys", Superalloys 1996, The Minerals, Metal and Material Society, 1996